SYNERGETIC EFFECT OF ZINC OXIDE, IRON OXIDE, AND BENTONITE/ZEOLITE P1 FOR THE EFFECTIVE CRYSTAL VIOLET REMOVAL BASED ON FENTON-LIKE OXIDATION

Tran Nguyen Phuong Lan[1], Ly Kim Phung[1]*, Nguyen Minh Nhut[1], Cao Luu Ngoc Hanh[1], Duong Thi My Tuyen[1], Tran Thanh Thao[2]

[1]*Can Tho University, Vietnam*

[2]*Vinh Long University of Technology and Education, Vietnam*

*Corresponding author: lkphung@ctu.edu.vn

(Received: September 12, 2025; Revised: November 10, 2025; Accepted: December 16, 2025)

DOI: 10.31130/ud-jst.2025.23(12).464E

Abstract - In this study, a ZnO/α-Fe_2O_3/bentonite/zeolite P1 (ZFBP) composite was successfully synthesised using natural bentonite sourced from Vietnam. The influence of zinc concentration on the Fenton-like catalytic efficiency toward crystal violet (CV) degradation and the physicochemical characteristics of ZFBP was evaluated through various analytical methods. At Fe_2O_3 and ZnO loadings of 15.14 wt.% and 7.34 wt.%, respectively, 92.54% degradation of CV was achieved in 40 min. Kinetic analysis revealed that the CV removal followed a pseudo-first-order model, with a reaction rate constant of 0.06 1/min under the optimal conditions. The removal mechanisms comprised of adsorption and the Fenton-like oxidation reaction, with the synergistic effect of the ZFBP components actively supporting the good removal efficiency. Furthermore, the composite demonstrated remarkable reusability after 10 cycles. These findings highlight the promising potential of ZFBP as an effective material for the treatment of organic dyes.

Key words - Bentonite; crystal violet; Fenton-like reaction; heterogeneous catalysts; ZnO and α-Fe_2O_3

1. Introduction

Industrial development plays a vital role in promoting social progress, but it also raises profound environmental challenges. The textile industry generates wastewater that contains high levels of toxic contaminants, posing a serious environmental risk [1, 2]. Crystal violet (CV), a cationic dye from the triarylmethane group, is widely applied in textile dyeing and cell staining [1]. Importantly, CV has been reported to negatively affect human health and organisms when exposed at high concentrations [2]. Accordingly, the development of effective strategies for CV removal has attracted more attention. Several current approaches include adsorption, advanced oxidation, and biotechnological methods. Among these, advanced oxidation processes have been attractive due to their high efficiency and reliability in the degradation of diverse pollutants [3]. The Fenton-like reaction is a representative example, employing iron oxide as a catalyst [2, 3]. Nevertheless, iron oxide is hindered by inherent drawbacks such as its relatively low surface area and strong tendency to agglomerate, which diminish catalytic efficiency. To address these limitations, a combination of the iron oxide and high surface area supports and other metal oxides, enhancing adsorption capacity and catalytic performance, is investigated [1-3].

Bentonite, a natural mineral available in Vietnam, possesses a layered tetrahedra and octahedra structure that provides effective adsorption capacity for heavy metals, dyes, and antibiotics [4]. Its performance can be enhanced by crystallizing zeolite on its surface to create a zeolite/bentonite composite [4]. Owing to the inherent iron content of bentonite, α-Fe_2O_3/bentonite/zeolite composites can be formed to provide catalytic performance for the Fenton-like oxidation reaction [5]. The addition of ZnO further enhances the catalytic efficiency of iron oxide through the synergistic effects [3, 6]. Therefore, the development of a composite composed of ZnO and α-Fe_2O_3/bentonite/zeolite (ZFBP) is promising for effective CV removal. This study aims to evaluate the role of zinc concentration on the physicochemical properties and catalytic activity of ZFBP. In addition, the effect of operational parameters on the CV degradation efficiency (catalyst dose, initial CV concentration, anion presence, scavenger presence, and reaction time) is also investigated. The pseudo-first-order (PFO) and pseudo-second-order (PSO) kinetic models are employed to propose removal mechanisms, and the ZFBP reusability is assessed to demonstrate its practical applications.

2. Materials and methods

2.1. Materials

Bentonite was collected in Lam Dong, Vietnam. Chemical reagents, namely sodium hydroxide (NaOH – 96%), zinc acetate dihydrate ($(CH_3COO)_2Zn.2H_2O$ – 99 %), hydrogen peroxide (H_2O_2 – 30%), and crystal violet ($C_{25}H_{30}N_3Cl$ – 88%) were purchased from Xilong, China.

2.2. Synthesis of ZFBP based on bentonite

In the first step, α-Fe_2O_3/bentonite/zeolite P1 (FBP) composite was created based on a previous study with some modifications [4]. Briefly, raw bentonite was calcined at 750°C for 1 h to produce activated bentonite. A mixture of 6 g of activated bentonite and 2 M NaOH solution was stirred in a two-necked flask at 70°C for 2 h, then heated to 100°C and maintained for 4 h. Finally, the solid was recovered by centrifugation, washed to neutral pH, and dried to constant weight to obtain the FBP composite. Subsequently, the ZFBP composite was prepared through the impregnation-precipitation [7]. FBP was impregnated with 50 mL of $(CH_3COO)_2Zn$ solution at different concentrations for 30 min, centrifuged, and dried to constant mass. The Zn^{2+}-loaded FBP was then reacted

with 0.5 M NaOH solution (a solid:liquid ratio of 1:50, w/v) at 80°C for 1h. The solid was separated using centrifugation, washed, and dried to constant mass. In this study, six zinc concentrations such as 0.31 mM (ZFBP1), 0.92 mM (ZFBP2), 1.54 mM (ZFBP3), 2.15 mM (ZFBP4). 2.77 mM (ZFBP5) and 3.69 mM (ZFBP6) were investigated.

2.3. Characterization of composite

This work used some advance analytical methods such as XRD, XRF, SEM, BET, and FTIR to characterize the physicochemical properties of composites. The characteristic peaks of composites were detected by a D8 diffractometer (Bruker, Germany) with CuKα radiation, 40 kV and 40 mA. An X-ray fluorescence spectrometer (XRF-1800, Shimadzu, Japan) was used to determine the chemical composition of composites. Meanwhile, the morphology of ZFBP was observed by an S-4800 scanning electron microscope instrument (Hitachi, Japan). The N_2 adsorption-desorption curve was measured at 77 K after degassing the composite at 473 K for 6 h, and the specific surface area and pore size of the composites were determined by the BET method. The characteristic vibration of ZFBP before and after use was collected by FTIR (Jasco FT/IR 4600, Japan).

2.4. The CV removal studies

The CV removal process using ZFBP composites was investigated at different operating conditions, including catalyst dose (0.125 – 0.75 g/L), initial CV concentration (150 – 375 mg/L), the presence of anions (Cl^-, NO_3^-, SO_4^{2-} and PO_4^{3-}) at concentration of 50 mM and the presence of scavengers (sodium oxalate, tert-butanol and isopropanol) at a concentration of 50 mM [8, 9]. Specifically, a precise amount of ZFBP was added to a mixture of 50 mL of 150 mg/L CV solution and 1 mL of 10 mM H_2O_2, shaking for 10 – 80 min. After the reaction, the liquid was separated from the suspension using a centrifuge. The initial CV solution and post solution after the reaction was measured by an UV-Visible Spectrophotometer (Multiskan SkyHigh, Thermo Fisher Scientific, USA) at λ_{max} = 590 nm. The removal efficiency (RE) was calculated based on the following formula:

$$RE\ (\%) = \frac{(C_0 - C_t)}{C_0} \times 100 \quad (1)$$

where C_0 and C_t are the initial concentration and the concentration at time t of CV solution, respectively. The mechanism of CV removal could be elucidated through fitting experimental data to the PFO and PSO kinetic models [2].

2.5. Reusability of composite

The reuse of ZFBP was evaluated under the optimal conditions for CV removal. A quantity of the used ZFBP composite was added an Erlenmeyer flask containing 50 mL of 225 mg/L CV solution and 1 mL of 10 mM H_2O_2, shaken for 40 min. After centrifugation, the remained concentration of CV in the solution was determined via the UV-vis method and the RE was calculated using formula (1). Meanwhile, the solid was washed with distilled water and dried for the next cycles of use.

3. Results and disscusion

3.1. Effect of zinc concentrations on the physicochemical properties of ZFBP composite

3.1.1. Evaluation of the CV removal ability

The effect of zinc concentration on CV removal using different methods, including adsorption (without H_2O_2) and Fenton-like reaction, is revealed in Figure 1. In the adsorption process, the RE of zinc-free FBP composite reached 39.69%; however, the incorporation of ZnO improved the RE due to the enhancement of adsorption sites [1], particularly giving 50% with ZFBP1. The increase of zinc concentrations could enhance the REs of ZFBP2 and ZFBP3 (54.20% and 56.11%), whereas the RE obtained 57.25% with ZFBP4. However, a further increase in zinc content (ZFBP5 and ZFBP6) led to the reduction in REs due to ZnO aggregation and blockage of active sites [1]. A similar trend was observed for the Fenton-like reaction, though overall RE values were higher. The FBP composite without zinc oxide exhibited an RE of 49.63%, which increased to 62.17% (ZFBP1) and peaked at 91.68% for ZFBP4, representing a 34.43% improvement compared to its adsorption performance. At the higher zinc oxide loadings, the RE slightly declined. Based on these results, ZFBP1, ZFBP4, and ZFBP6 were selected for analyzing the physicochemical characterization.

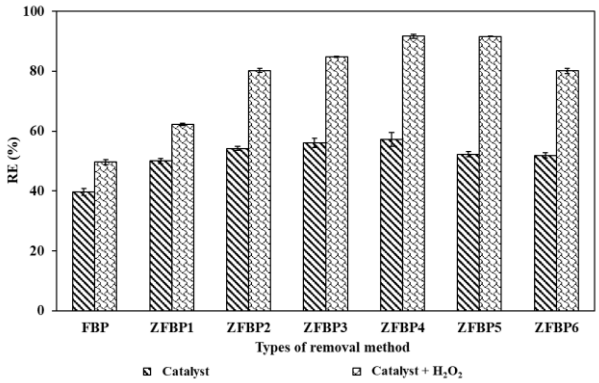

Figure 1. *The CV removal ability of composites based on different methods: catalyst and catalyst + H_2O_2*

3.1.2. X-Ray diffraction

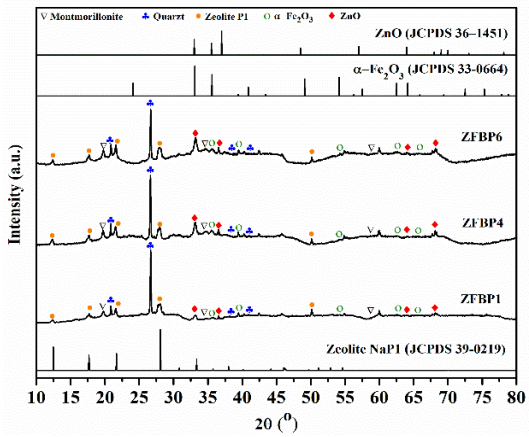

Figure 2. *XRD patterns of the composites*

The XRD patterns of ZFBP1, ZFBP4, ZFBP6, and the standard cards of zeolite P1, α-Fe_2O_3, and ZnO are shown

in Figure 2. Phases corresponding to bentonite and zeolite P1 were clearly identified, with quartz and montmorillonite phases observed at 2θ angles of 21.56°, 26.63°, 37.67°, 41.91° and 22.76°, 34.62°, 59.67°, respectively [4]. Meanwhile, the additional peaks of 12.46°, 17.66°, 21.67°, 28.10°, 52.89° confirmed the crystallization of zeolite P1 on the bentonite support [4]. The catalytic components such as α-Fe_2O_3 and ZnO were identified at peaks 35.61°, 40.91°, 54.12°, 62.52°, 65.91° and 33.50°, 34.99°, 62.02°, 66.01°, respectively [10, 11]. Upon an increase in the zinc concentration, stronger ZnO signals resulted, particularly at 33°, indicating higher ZnO content in the composites.

3.1.3. Chemical composition

The chemical compositions of FBP and ZFBP composites are shown in Table 1. FBP primarily contained bentonite- and zeolite-related phases, with the formation of zeolite P1 confirmed by a SiO_2/Al_2O_3 molar ratio of 3.64 [12]. The ZFBP composites exhibited similar SiO_2, Al_2O_3, and Fe_2O_3 contents to the FBP composites, indicating structural stability after the ZnO incorporation. The main compositional variations were observed in Na_2O and ZnO contents. A significant decrease in Na_2O content (from 11.72% to 0.37%) with increasing ZnO can be explained by the attachment of Zn^{2+} ions to the FBP matrix, which mainly occured based on the adsorption and ion exchange mechanism between Zn^{2+} and Na^+ ions [10]. ZFBP1 contained 3.27% ZnO, which synergistically interacted with Fe_2O_3 to enhance the Fenton-like CV degradation [1, 3]. With higher zinc loading, the ZnO content increased to 7.34% (ZFBP4) and 9.11% (ZFBP6), providing more active sites for the adsorption and oxidation [3, 10]. However, excessive ZnO promoted aggregation with Fe_2O_3, diminishing catalytic synergy [1]. Among them, ZFBP4 exhibited the most favorable composition and the highest CV removal ability; therefore, further characterization focused on this composite.

Table 1. *Chemical composition of ZFBP composites*

Chemical composition (%)	Sample			
	FBP	ZFBP1	ZFBP4	ZFBP6
SiO_2	47.61	52.41	50.02	50.34
Al_2O_3	22.24	24.02	22.42	23.09
Fe_2O_3	14.50	15.53	15.14	15.32
Na_2O	11.72	2.92	3.29	0.37
ZnO	-	3.27	7.34	9.11
Others	3.93	1.88	1.79	1.77

3.1.4. Surface morphology of composite

The morphology of ZFBP4 was characterized by crystalline zeolite P1 particles on bentonite; meanwhile, the smaller ZnO and Fe_2O_3 particles (an area circled in red) were scattered on both bentonite and zeolite P1 (Figure 3). The more abundant sites found in SEM images promoted more CV molecules to be adsorbed on ZFBP4. Similar crystalline zeolite morphologies on bentonite substrates have been previously reported [4], along with the incorporation of metal oxides in ZnO/bentonite [11] and ZnO/zeolite composites [13].

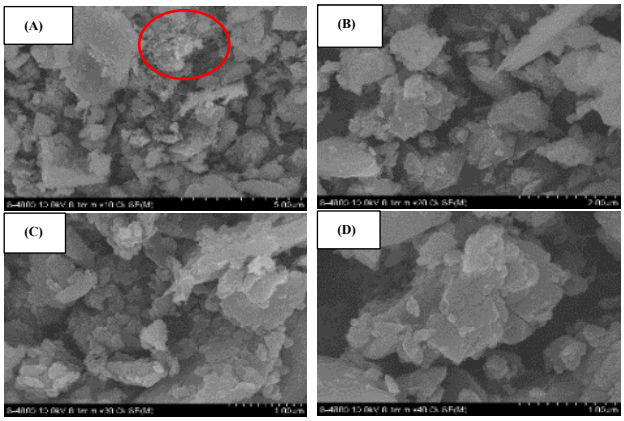

Figure 3. *SEM images of ZFBP4 at different magnifications: (A) 10000, (B) 20000, (C) 30000, and (D) 40000*

3.1.5. Texture properties

The texture properties of ZFBP4, including specific surface area, pore volume, and pore size were 74 m^2/g, 0.071 cm^3/g, and 3.81 nm, respectively. As shown in Figure 4, the N_2 adsorption-desorption isotherm corresponded to type IV (IUPAC), with an H3 hysteresis loop in the relative pressure range of 0.4 – 0.9, confirming a mesoporous structure with slit-like pores formed by stacked bentonite layers [10, 14]. A mesopore further facilitated the diffusion of bulky dye molecules toward the active sites of the composite surface. The isoelectric point of ZFBP4 was 6.8, indicating that the composite surface is negatively charged at pH>6.8 and vice versa. Consequently, the CV removal in this work was operated at pH 7.

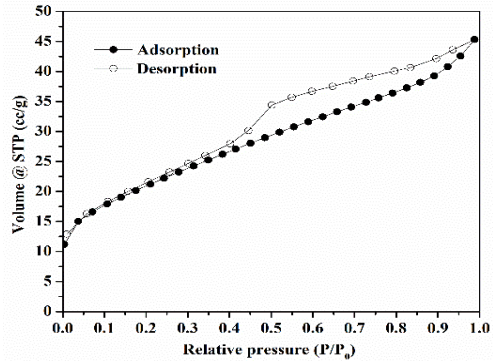

Figure 4. *N_2 adsorption-desorption curve of ZFBP4*

3.2. Effect of operating conditions onto the CV removal of ZFBP composite

3.2.1. Effect of catalyst dose

The catalyst dose significantly affected the CV removal of the ZFBP4 composite. Experiments were conducted with the catalyst dose varying from 0.125 to 0.75 g/L under the fixed conditions such as pH 7, an initial CV concentration of 150 mg/L, a H_2O_2 concentration of 10 mM, and the reaction time of 10 – 80 min (Figure 5A). Within the first 10 min, RE markedly increased with catalyst loading, reaching 39.88% at 0.125 g/L, and rising to 45.48%, 57.04%, and 76.20% at two-, four-, and sixfold higher doses, respectively. A similar trend was observed between 10 and 40 min, attributed to the large number of active sites, generating more Fe^{2+} and Zn^{2+} ions, which

catalyzed the production of the free radicals to decompose CV molecules [2, 15]. Prolonging the reaction time to beyond 40 min, the RE approached equilibrium at catalyst doses of 0.25-0.75 g/L, while 0.125 g/L required about 60 min to achieve the equilibrium. With high RE (98.55%) after 40 min, the catalyst dose of 0.25 g/L was chosen to limit catalyst waste.

3.2.2. Effect of the initial CV concentration

The effect of initial CV concentration in the range of 150 – 375 mg/L was carried out at pH 7, a catalyst dose of 0.25 g/L, H_2O_2 concentration of 10 mM from 10 – 80 min. The REs significantly decreased with an increase in the initial CV concentrations from 225 to 375 mg/L (Figure 5B). This decline was attributed to the competitive occupation of active sites and reduced the interaction between H_2O_2 and catalyst sites, limiting the free radical production [2]. Additionally, more CV was used at the fixed amount of H_2O_2 and catalyst, causing insufficient reagents for oxidative [3]. Nevertheless, after 40 min, high REs of 92.54% and 85.04% obtained at 225 mg/L and 300 mg/L, respectively, demonstrating the strong catalytic performance of ZFBP4.

3.2.3. Effect of anion

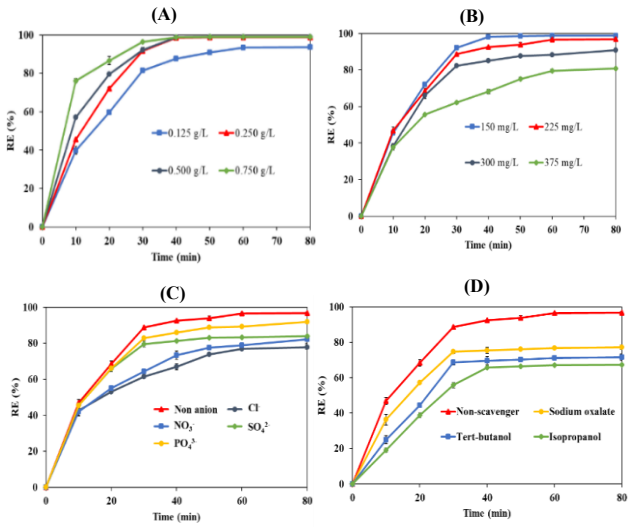

Figure 5. *The CV removal of ZFBP4 at different conditions: catalyst dose (A), initial CV concentration (B), the presence of anions (C); and the presence of scavengers (D)*

Common anions present in water sources can affect the CV removal of ZFBP4. At pH 7, a catalyst dose of 0.25 g/L, an initial CV concentration of 150 mg/L, the H_2O_2 concentration of 10 mM, and a reaction time of 10 – 80 min, the effects of anions such as Cl^-, NO_3^-, SO_4^{2-}, and PO_4^{3-} were investigated (Figure 5C). In the presence of both SO_4^{2-} and PO_4^{3-} anions, REs slightly reduced to 81.29% and 86.02% after 40 min, respectively. In contrast, Cl^- and NO_3^- exhibited stronger inhibition of free radical production in the reaction system, resulting in a decrease in REs to 66.99% and 73.36%, respectively. The strong influence of the Cl^- anions was attributed to their scavenging of $^{\bullet}OH$ radicals, while NO_3^- and SO_4^{2-} might also generate less reactive nitrate and sulfate radicals [16, 17]. Meanwhile, PO_4^{3-} anions may form iron-related complexes on the catalyst surface, limiting the interaction of H_2O_2-catalytic sites [16]. Despite these effects, REs remained within 70 – 85%, highlighting the potential of composites in practical wastewater treatment.

3.2.4. Effect of scavengers

The effect of radical scavengers, including sodium oxalate, tert-butanol, and isopropanol on CV removal was investigated at pH 7, a catalyst dose of 0.25 g/L, and an initial CV concentration of 225 mg/L. The RE significantly decreased in the presence of these scavengers. Specifically, the RE dropped to 75.38%, 69.56%, and 65.84% in the presence of sodium oxalate, tert-butanol, and isopropanol, respectively, compared to the absence of scavengers (92.54%). The more pronounced reductions observed with tert-butanol and isopropanol indicated that $^{\bullet}OH$ radicals were the main reactive species responsible for the oxidation of CV molecules [8, 9]. The greater decrease in RE with isopropanol suggested that CV molecules were primarily degraded by $^{\bullet}OH$ radicals in the solution rather than those generated on the ZFBP4 surface [9]. Besides, the less effect of sodium oxalate implied that photocatalytic oxidation was not the dominant pathway in this process [8]. These findings proposed that free $^{\bullet}OH$ radicals in the medium generated from the Fenton-like reactions on the ZFBP4 surface can simultaneously degrade CV molecules adsorbed on the catalyst surface.

3.2.5. Kinetics of CV removal

Table 2 revealed that the correlation coefficient (R^2) of the PFO model is higher than that of the PSO model at all CV concentrations, implying that the experimental reaction process mainly followed the PFO model.

Table 2. *Kinetic parameters of the CV removal process*

Initial CV concentration (mg/L)	PFO model		PSO model	
	k_1 (1/min)	R^2	k_2 (L/mg.min)	R^2
150	0.091	0.994	0.077	0.970
225	0.060	0.997	0.060	0.988
300	0.043	0.987	0.033	0.952
375	0.024	0.990	0.034	0.955

The reaction rate constant decreased from 0.091 to 0.024 1/min, corresponding to an increase in the CV concentration from 150 to 375 mg/L. The good agreement with the PFO model suggested that the reaction process is significantly affected by the pollutant concentrations, whereas the amount of catalyst and free radicals generated from the active sites is stable and abundant [2, 10].

3.2.6. Reutilization of ZFBP4 composite

The reusability of the ZFBP4 composite was assessed at pH 7, a catalyst dose of 0.25 g/L, an initial CV concentration of 225 mg/L, and the H_2O_2 concentration of 10 mM during 40 min (Figure 6). The REs of ZFBP4 after the 2nd and 3rd cycles still reached 91.18% and 89.05%, respectively. In the following cycles, the RE significantly dropped to 78.07% and 61.93% at the 6th and 10th cycles, respectively. The difference in RE between the first and last uses was about 30.6%, demonstrating the potential regeneration of the ZFBP4 composite over multiple cycles.

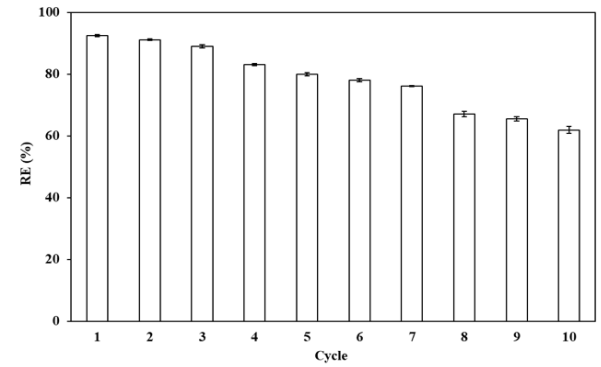

Figure 6. *The CV removal cycles of the ZFBP4 composite*

Based on the BET results of ZFBP4 composite after 10 cycles, the specific surface area, pore volume, and pore size were 8 m^2/g, 0.024 cm^3/g, and 1.32 nm, respectively. The decrease in these values exhibited the possibility of pore-filling and catalyst deactivation of ZFBP4 that occurred after recycling, resulting in the reduction in RE for CV dye.

3.2.7. The proposed removal mechanism

Figure 7 indicated the FTIR spectrum of ZFBP4 before and after the Fenton-like reaction. For the fresh composite, the broad peak at 3293.29 cm^{-1} represented the –OH group of water molecules adsorbed on ZFBP4 [18]. The bending vibration of –OH group and the stretching vibration of Si-O-Si (or Si-O-Al) of bentonite and zeolite P1 could be detected at 1667.98 cm^{-1} and 998.76 cm^{-1}, respectively [4, 18]. The presence of quartz phase was also noted at 797.40 cm^{-1} and 668.85 cm^{-1} [18]. The stretching vibrations of Fe-O and Zn-O bonds were detected at 566.71 cm^{-1} and 467.00 cm^{-1}, respectively [19, 20].

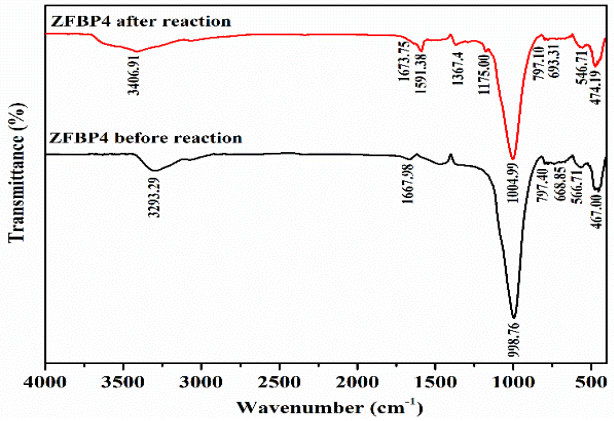

Figure 7. *FTIR spectrum of ZFBP4 before and after the reaction*

After the reaction, the characteristic vibrations of the composite were still maintained, demonstrating the stability of the ZFBP4 composite. New vibrations were detected at 1591.38 cm^{-1} and 1367.4 cm^{-1}, which belonged to the stretching vibrations of -C=C and -N–H, respectively [21], indicating the successful CV capture on the composite surface. The CV removal mechanism of the composite included the adsorption and the Fenton-like reaction. In the initial stage, the CV molecules and H_2O_2 diffused from the solution into the composite surface [10]. After adsorption, the reactants existed around Fe_2O_3 and ZnO, and the free radicals could be generated from the reaction between Fe^{2+} and H_2O_2 [2, 10]. Meanwhile, ZnO played a role in promoting the conversion from Fe^{3+} to Fe^{2+} [3]. The synergistic effect of the phase components of ZFBP4 assisted to decompose CV into intermediate products.

The RE of CV depended on the original source of the catalyst (Table 3). A catalyst of Zn^0/Fe_3O_4 exhibited a remarkable synergistic effect with the RE of 95% within 10 min [15]; however, its activity was restricted at the higher CV concentrations because of the limited surface area and number of active sites. In contrast, iron oxide supported on activated carbon and Fe/Ni immobilized on bentonite/fly ash/algae exhibited the superior catalytic performance which could maintain the REs above 90% at concentrations of 400–1000 mg/L [1, 2]. Compared to these catalysts, ZFBP4 demonstrated the competitive RE, achieving 92.54% at 225 mg/L under the milder operating conditions (neutral pH, low catalyst dose of 0.25 g/L, and 40 min), indicating that ZFBP4 is capable of more practical conditions.

Table 3. *The CV removal performance of the ZFBP4 composite and previous materials*

Types of catalyst	Reaction condition	RE (%)	Ref.
Zn^0/Fe_3O_4	pH 5.0, dose of 1.0 g/L, [a][CV] of 15 mg/L, [b][H_2O_2] of 0.68 mM, 10 min	95.00	[15]
Fe/Clay	pH 7.0, dose of 0.75 g/L, [a][CV] of 20 mg/L, [b][H_2O_2] of 100 mM, 10 min	99.00	[22]
Iron oxide/activated carbon	pH 7.7, dose of 1.7 g/L, [a][CV] of 400 and 1000 mg/L, [b][H_2O_2] of 123 mM, 120 min	99.70 (400 mg/L) 91.86 (1000 mg/L)	[1]
Fe/Ni based on bentonite/fly ash/algae	pH 7.0, dose of 0.2 g/L, [a][CV] of 1000 mg/L, [b][H_2O_2] of 50 mM, 120 min	91.86	[2]
ZFBP4	pH 7.0, dose of 0.25 g/L, [a][CV] of 225 mg/L, [b][H_2O_2] of 10 mM, 40 min	92.54	This study

[a][CV]: initial CV concentration; [b][H_2O_2]: H_2O_2 concentration

4. Conclusion

ZFBP4 composite synthesized from bentonite exhibited the high efficiency in CV removal due to the synergistic effect of zinc oxide and iron oxide. The composite exposed the best catalytic performance with the composite content of SiO_2 (50.02%), Al_2O_3 (22.42%), Fe_2O_3 (15.14%), Na_2O (3.29%), and ZnO (7.34%). The RE reached the optimal of 92.54% at a catalyst dose of 0.25 g/L, initial CV concentration of 225 mg/L, H_2O_2 concentration of 10 mM in 40 min. The experimental data were consistent with the PFO kinetic (R^2 = 0.997). Furthermore, the durability of ZFBP4 composite was determined, with RE decreasing by about 30.6% after 10 regeneration cycles. These findings suggested that the ZFBP4 composite is a potential catalyst for the CV dye removal in real wastewater sources.

REFERENCES

[1] L. Wang *et al.*, "Catalytic degradation of crystal violet and methyl orange in heterogeneous Fenton-like processes", *Chemosphere*, vol. 344, 140406, 2023.

[2] J. Liu, Y. Du, W. Sun, Q. Chang, and C. Peng, "Preparation of new adsorbent-supported Fe/Ni particles for the removal of crystal violet and methylene blue by a heterogeneous Fenton-like reaction", *RSC Advances*, vol. 9, pp. 22513-22522, 2019.

[3] G. Ren, K. Zhao, and L. Zhao, "A Fenton-like method using ZnO doped MIL-88A for degradation of methylene blue dyes", *RSC Advances*, vol. 10, pp. 39973-39980, 2020.

[4] M. R. Abukhadra, S. M. Ali, E. A. Nasr, H. A. A. Mahmoud, and E. M. Awwad, "Effective sequestration of phosphate and ammonium ions by the bentonite/zeolite Na–P composite as a simple technique to control the eutrophication phenomenon: realistic studies", *ACS Omega*, vol. 5, pp. 14656-14668, 2020.

[5] J. S. Al-Jariri and F. Khalili, "Adsorption of Zn(II), Pb(II) and Mn(II) from water by Jordanian bentonite", *Desalination and Water Treatment*, vol. 21, pp. 308-322, 2010.

[6] A. Nath, D. K. Mahato, L. R. Singh, P. K. Kuiri, and M. Mahato, "Waste-derived green ZnO–Fe_2O_3 photocatalyst for degradation of MB dye pollutant in water", *Inorganic and Nano-Metal Chemistry*, vol. 55, pp. 178-191, 2025.

[7] M. Jyoti, D. Vijay, and S. Radha, "To study the role of temperature and sodium hydroxide concentration in the synthesis of zinc oxide nanoparticles", *International Journal of Scientific and Research Publications*, vol. 3, pp. 1-4, 2013.

[8] Y. Guan *et al.*, "One-dimensional photocatalysts of AVO_4 (A = Bi, Fe)/carbon nanofibers frameworks: an alternative strategy in improving photocatalytic activities", *Journal of Materials Science: Materials in Electronics*, vol. 29, pp. 11852–11861, 2018.

[9] C. Cai, Z. Zhanga, J. Liua, N. Shana, H. Zhanga, and D. D. Dionysiou, "Visible light-assisted heterogeneous Fenton with $ZnFe_2O_4$ for the degradation of Orange II in water", *Applied Catalysis B: Environmental*, vol. 182, pp. 456-468, 2016.

[10] P. L. Tran-Nguyen *et al.*, "Iron oxides/zeolite X composite derived from rice husk ash: fabrication and physicochemical properties for superior heterogeneous Fenton-like oxidation of crystal violet", *Journal of Chemical Technology & Biotechnology*, vol. 100, pp. 1222-1237, 2025.

[11] M. Alshabanat *et al.*, "Preparation and characterization of ZnO/bentonite nanocomposites for enhanced photocatalytic degradation of pesticides in contaminated water", *Scientific Reports*, vol. 15, 23816, 2025.

[12] P. L. Tran-Nguyen *et al.*, "Evaluation of the potential removal of phosphate using rice husk ash-derived zeolite NaP1", *Journal of Chemical Technology & Biotechnology*, vol. 98, pp. 1465-1477, 2023.

[13] S. Sarabyar, A. Farahbakhsh, H. A. Tahmasebi, B. M. Vaziri, and S. Khosroyar, "Enhancing photocatalytic degradation of beta-blocker drugs using TiO_2 NPs/zeolite and ZnO NPs/zeolite as photocatalysts: optimization and kinetic investigations", *Scientific Reports*, vol. 14, 27390, 2024.

[14] H. Asnaoui, Y. Dehmani, M. Khalis, and H. El-Kaber, "Adsorption of phenol from aqueous solutions by Na–bentonite: kinetic, equilibrium and thermodynamic studies", *International Journal of Environmental Analytical Chemistry*, vol. 102, pp. 3043-3057, 2022.

[15] H. Tian *et al.*, "A new Fenton-like system for catalytic oxidation of crystal violet using Zn^0/Fe_3O_4", *Desalination and Water Treatment*, vol. 110, pp. 219-228, 2018.

[16] J. Wang and S. Wang, "Effect of inorganic anions on the performance of advanced oxidation processes for degradation of organic contaminants", *Chemical Engineering Journal*, vol. 411, 128392, 2021.

[17] Y. Deng, E. Rosario-Muniz, and X. Ma, "Effects of inorganic anions on Fenton oxidation of organic species in landfill leachate", *Waste Management and Research*, vol. 30, pp. 12-19, 2017.

[18] Y. S. Chang *et al.*, "Adsorption of Cu(II) and Ni(II) ions from wastewater onto bentonite and bentonite/GO composite", *Environmental Science and Pollution Research*, vol. 27, pp. 33270-33296, 2020.

[19] M. Liu, S. Yu, H. Li-an, and X. Hu, "Removal of oxytetracycline by Fe_2O_3–TiO_2/modified zeolite composites under visible light irradiation", *Journal of Materials Science: Materials in Electronics*, vol. 30, pp. 9087-9096, 2019.

[20] H. N. Ulya, A. Taufiq, and Sunaryono, "Comparative structural properties of nanosized ZnO/Fe_3O_4 composites prepared by sonochemical and sol-gel methods", *International Conference on Life Sciences and Technology*, vol. 276, 012059, 2019.

[21] E. B. Onuk and B. Isik, "Adsorptive removal of toxic methylene blue and crystal violet dyes from aqueous solutions using *Prunus spinosa*: isotherm, kinetic, thermodynamic, and error analysis", *Biomass Conversion and Biorefinery*, vol. 15, pp. 19805-19822, 2025.

[22] M. Idrissi, Y. Miyah, Y. Benjelloun, and M. Chaouch, "Degradation of crystal violet by heterogeneous Fenton-like reaction using Fe/Clay catalyst with H_2O_2", *Journal of Materials and Environmental Science*, vol. 7, no. 1, pp. 50-58, 2016.